

# Plasma modelling using FEniCS and FEDM

A. P. Jovanović, D. Loffhagen, and M. M. Becker

Leibniz Institute for Plasma Science and Technology (INP)  
Felix-Hausdorff-Str. 2, 17489 Greifswald

*FEniCS 2021*  
*25 March 2021*



Funded by the Deutsche  
Forschungsgemeinschaft -  
project number 407462159

- Plasma is a gaseous state in which free electrons and ionised atoms or molecules exist.
- Non-thermal low-temperature plasmas considered here are usually produced by electric discharges.
- They are used for different applications, such as chemical and surface processing, or biomedical applications.
- In order to describe physical and chemical processes in plasma, experimental studies are often supplemented by numerical modelling.



*Images obtained from <https://www.inp-greifswald.de/>*

## Introduction

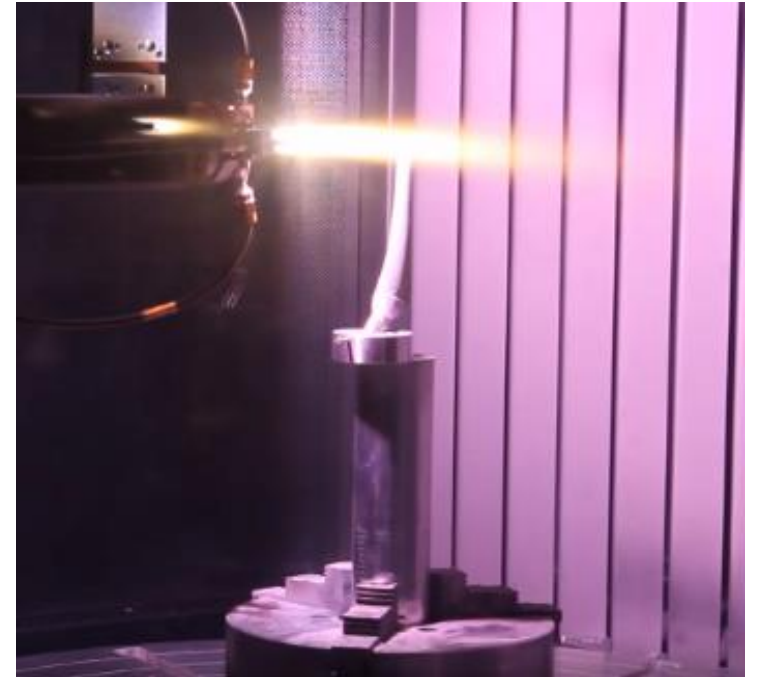
- Plasma is a gaseous state in which free electrons and ionised atoms or molecules exist.
- Non-thermal low-temperature plasmas considered here are usually produced by electric discharges.
- They are used for different applications, such as chemical and surface processing, or biomedical applications.
- In order to describe physical and chemical processes in plasma, experimental studies are often supplemented by numerical modelling.



*Images obtained from <https://www.inp-greifswald.de/>*

## Introduction

- Plasma is a gaseous state in which free electrons and ionised atoms or molecules exist.
- Non-thermal low-temperature plasmas considered here are usually produced by electric discharges.
- They are used for different applications, such as chemical and surface processing, or biomedical applications.
- In order to describe physical and chemical processes in plasma, experimental studies are often supplemented by numerical modelling.



*Images obtained from <https://www.inp-greifswald.de/>*

## Introduction

- Plasma is a gaseous state in which free electrons and ionised atoms or molecules exist.
- Non-thermal low-temperature plasmas considered here are usually produced by electric discharges.
- They are used for different applications, such as chemical and surface processing, or biomedical applications.
- In order to describe physical and chemical processes in plasma, experimental studies are often supplemented by numerical modelling.



*Images obtained from <https://www.inp-greifswald.de/>*

# Governing equations

- Poisson's equation for electric potential

$$-\varepsilon_0 \varepsilon_r \nabla^2 \phi = \sum_p q_p n_p$$

$$\mathbf{E} = -\nabla \phi$$

- Electron energy balance equation

$$\frac{\partial w_e}{\partial t} + \nabla \cdot \mathbf{Q}_e = -e_0 \mathbf{E} \cdot \mathbf{\Gamma}_e + \tilde{S}_e$$

$$\mathbf{Q}_e = -\frac{5}{3} b_e \mathbf{E} w_e - \nabla \left( \frac{5}{3} D_e w_e \right)$$

$$\tilde{S}_e = \sum_{j=1}^{N_r} \Delta \varepsilon_j R_j$$

- Continuity equation for particle densities

$$\frac{\partial n_p}{\partial t} + \nabla \cdot \mathbf{\Gamma}_p = S_p$$

$$\mathbf{\Gamma}_p = \text{sgn}(q_p) b_p \mathbf{E} n_p - \nabla (D_p n_p)$$

$$S_p = \sum_{j=1}^{N_r} (G_{pj} - L_{pj}) k_j \prod_{i=1}^{N_s} n_i^{\beta_{ij}}$$

- In order to solve the equations, appropriate set of boundary conditions is used:
  - Dirichlet and Robin boundary conditions for Poisson's equation
  - Robin boundary conditions for continuity equations, and electron energy balance equation.

# Challenges in plasma modelling

- For appropriate description of the processes in plasma, lots of particles, and consequently, lots of processes need to be taken into account.

**Table 1** Collision processes related to TMS included in the basic reaction kinetics model in addition to the argon model reported in [34]

Index	Reaction	Rate coefficient	References
<i>Elastic electron collisions</i>			
1	$(\text{CH}_3)_2\text{Si} + e \rightarrow (\text{CH}_3)_2\text{Si} + e$	$f(u_e)$	[45]
<i>Electron impact excitation and dissociation</i>			
2	$(\text{CH}_3)_2\text{Si} + e \rightarrow (\text{CH}_3)_2\text{Si}[v_1] + e$	$f(u_e)$	[45]
3	$(\text{CH}_3)_2\text{Si} + e \rightarrow (\text{CH}_3)_2\text{Si}[v_2] + e$	$f(u_e)$	[45]
4	$(\text{CH}_3)_4\text{Si} + e \rightarrow (\text{CH}_3)_3\text{Si} + \text{CH}_3 + e$	$f(u_e)$	[20, 45]
<i>Electron impact ionization and detachment</i>			
5	$(\text{CH}_3)_4\text{Si} + e \rightarrow (\text{CH}_3)_3\text{Si}^+ + \text{CH}_3 + 2e$	$f(u_e)$	[46]
6	$(\text{CH}_3)_3\text{Si}^- + e \rightarrow (\text{CH}_3)_3\text{Si} + 2e$	$f(u_e)$	[47–49]
<i>Dissociative electron attachment</i>			
7	$(\text{CH}_3)_4\text{Si} + e \rightarrow (\text{CH}_3)_3\text{Si}^- + \text{CH}_3$	$f(u_e)$	[45]
<i>Ion-molecule reactions</i>			
8	$\text{Ar}^+ + (\text{CH}_3)_4\text{Si} \rightarrow (\text{CH}_3)_3\text{Si}^+ + \text{CH}_3 + \text{Ar}[1p_0]$	$1.5 \times 10^{-15}$	[36, 50]
9	$\text{Ar}_2^+ + (\text{CH}_3)_4\text{Si} \rightarrow (\text{CH}_3)_3\text{Si}^+ + \text{CH}_3 + 2 \text{Ar}[1p_0]$	$1.2 \times 10^{-15}$	[36, 50]
<i>Quenching of excited argon species leading to Penning ionization</i>			
10–16	$\text{Ar}^* + (\text{CH}_3)_4\text{Si} \rightarrow (\text{CH}_3)_3\text{Si}^+ + \text{CH}_3 + \text{Ar}[1p_0] + e$	$k_{M,Ar}^{PI}$	See text
<i>Quenching of excited argon species leading to neutral products</i>			
17–23	$\text{Ar}^* + (\text{CH}_3)_4\text{Si} \rightarrow (\text{CH}_3)_3\text{Si} + \text{CH}_3 + \text{Ar}[1p_0]$	$k_{M,Ar}^Q$	See text
24–27	$\text{Ar}_2^* + (\text{CH}_3)_4\text{Si} \rightarrow (\text{CH}_3)_3\text{Si} + \text{CH}_3 + 2 \text{Ar}[1p_0]$	$k_{M,Ar}^A$	Analogous to $\text{Ar}^*$ [51, 52]

D. Loffhagen et al., *Plasma Chem. Plasma Process.* **41** (2021) 289

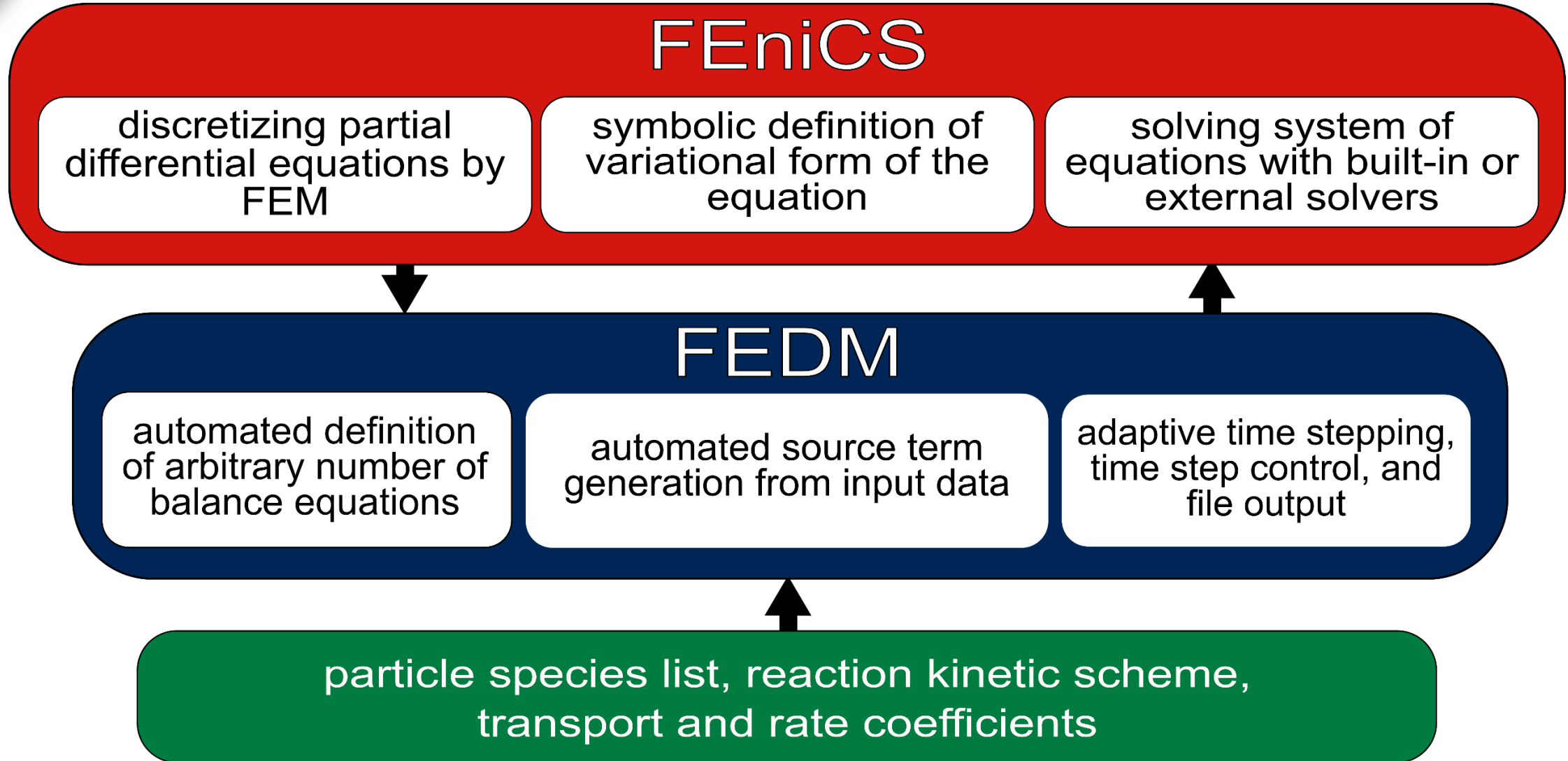
- Chemical reactions in plasma model usually lead to stiff system of equations.
- Time scale of the problem spans from picoseconds to tens of seconds.

Springer

**Table 2** (continued)

Index	Reaction	Rate coefficient	References
552	$\text{CH}_4 + \text{C}_2\text{H} \rightarrow \text{C}_2\text{H}_2 + \text{CH}_3$	$2.3 \times 10^{-18}$	[130]
553	$\text{CH}_4 + \text{C}_2 \rightarrow \text{C}_2\text{H} + \text{CH}_3$	$1.7 \times 10^{-17}$	[131]
554	$\text{CH}_4 + \text{CH} \rightarrow \text{C}_2\text{H}_4 + \text{H}$	$9.0 \times 10^{-17}$	[132]
555	$\text{C}_2\text{H}_6 + \text{C}_2\text{H} \rightarrow \text{C}_2\text{H}_2 + \text{C}_2\text{H}_4$	$3.5 \times 10^{-17}$	[133]
556	$\text{C}_2\text{H}_6 + \text{C}_2 \rightarrow \text{C}_2\text{H} + \text{C}_2\text{H}_4$	$1.6 \times 10^{-16}$	[134]
557	$\text{C}_2\text{H}_6 + \text{CH} \rightarrow \text{C}_2\text{H}_4 + \text{CH}_3$	$1.3 \times 10^{-16}$	[129]
558	$\text{C}_2\text{H}_6 + \text{CH} \rightarrow \text{C}_3\text{H}_6 + \text{H}$	$3.0 \times 10^{-17}$	[129]
559	$\text{C}_2\text{H}_2 + \text{C}_2\text{H}_3 (+M) \rightarrow \text{C}_4\text{H}_5 (+M)$	$1.9 \times 10^{-17}$	[126]
560	$\text{C}_2\text{H}_2 + \text{C}_2\text{H}_3 \rightarrow \text{C}_2\text{H}_6 + \text{C}_2\text{H}_4$	$2.4 \times 10^{-18}$	[126]
561	$\text{C}_2\text{H}_2 + \text{C}_2\text{H}_3 (+M) \rightarrow \text{C}_4\text{H}_4 (+M)$	$2.5 \times 10^{-17}$	[135]
562	$\text{C}_2\text{H}_2 + \text{C}_2\text{H}_3 \rightarrow 2\text{C}_2\text{H}_4$	$8.0 \times 10^{-19}$	[135]
563	$\text{C}_2\text{H}_2 + \text{C}_2\text{H}_3 \rightarrow \text{C}_2\text{H}_6 + \text{C}_2\text{H}_2$	$8.0 \times 10^{-19}$	[135]
564	$\text{C}_2\text{H}_2 + \text{CH}_3 \rightarrow \text{CH}_3 + \text{C}_2\text{H}_4$	$3.0 \times 10^{-17}$	[135]
565	$\text{C}_2\text{H}_2 + \text{H} \rightarrow 2\text{CH}_3$	$6.0 \times 10^{-17}$	[126]
566	$\text{C}_2\text{H}_2 + \text{C}_2\text{H} \rightarrow \text{C}_2\text{H}_2 + \text{C}_2\text{H}_3$	$1.2 \times 10^{-16}$	[133]
567	$\text{C}_2\text{H}_2 + \text{C}_2 \rightarrow 2\text{C}_2\text{H}_2$	$3.3 \times 10^{-16}$	[134]
568	$\text{C}_2\text{H}_2 + \text{H} (+M) \rightarrow \text{C}_2\text{H}_2 (+M)$	$1.1 \times 10^{-18}$	[126, 127]
569	$\text{C}_2\text{H}_2 + \text{C}_2\text{H}_3 (+M) \rightarrow \text{C}_4\text{H}_6 (+M)$	$1.6 \times 10^{-17}$	[135]
570	$\text{C}_2\text{H}_2 + \text{C}_2\text{H}_3 \rightarrow \text{C}_2\text{H}_4 + \text{C}_2\text{H}_2$	$1.6 \times 10^{-18}$	[135]
571	$\text{C}_2\text{H}_2 + \text{CH}_3 \rightarrow \text{CH}_3 + \text{C}_2\text{H}_2$	$3.0 \times 10^{-17}$	[135]
572	$\text{C}_2\text{H}_2 + \text{H} \rightarrow \text{C}_2\text{H}_2 + \text{H}_2$	$2.0 \times 10^{-17}$	[126]
573	$\text{C}_2\text{H} + \text{CH}_2 \rightarrow \text{CH} + \text{C}_2\text{H}_2$	$3.0 \times 10^{-17}$	[135]
574	$\text{C}_2\text{H} + \text{H} (+M) \rightarrow \text{C}_2\text{H}_2 (+M)$	$3.0 \times 10^{-16}$	[135]
575	$\text{C}_2 + \text{H}_2 \rightarrow \text{C}_2\text{H} + \text{H}$	$1.5 \times 10^{-18}$	[136]

# FEDM (Finite Element Discharge Modelling) code



# FEDM (Finite Element Discharge Modelling) code

- Transport and reaction rate coefficients are imported into model in form of functions or look-up tables.
- Source term definition is automated based on the reaction kinetic scheme.
- Time discretization is done using backward differentiation formula.

$$y_{n+2} - \frac{(1+\omega_{n+1})^2}{1+2\omega_{n+1}} y_{n+1} + \frac{\omega_{n+1}^2}{1+2\omega_{n+1}} y_n = \Delta t_{n+2} \frac{1+\omega_{n+1}}{1+2\omega_{n+1}} f_{n+2}$$

- Time stepping control is done using either *H211b* or *PI.3.4* controllers.

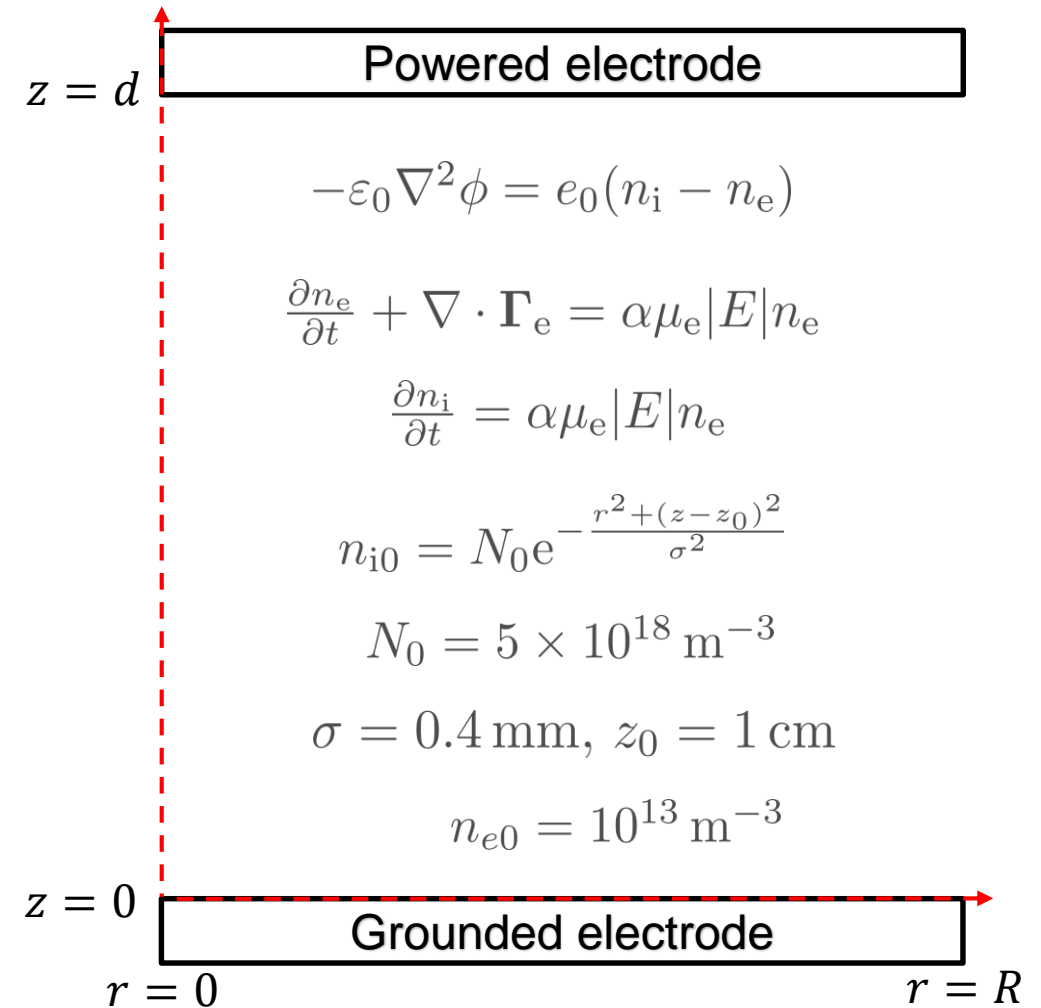
$$\Delta t_{n+1} = \left( \frac{0.8TOL}{\hat{r}_{n+1}} \right)^{0.3/k} \left( \frac{\hat{r}_n}{\hat{r}_{n+1}} \right)^{0.4/k} \Delta t_n$$

$$\Delta t_{n+1} = \left( \frac{0.8TOL}{\hat{r}_n} \right)^{0.25/k} \left( \frac{0.8TOL}{\hat{r}_{n-1}} \right)^{0.25/k} \left( \frac{\Delta t^n}{\Delta t^{n-1}} \right)^{-0.25} \Delta t^n$$

*E. Alberdi Celaya et al., Procedia Comput. Sci., 29, 1014–1026 (2014)*  
*G. Söderlind and L. Wang, J. Comput. Appl. Math., 185, 225–243 (2006)*  
*G. Söderlind, Numer. Algorithms, 31, 281–310 (2002)*

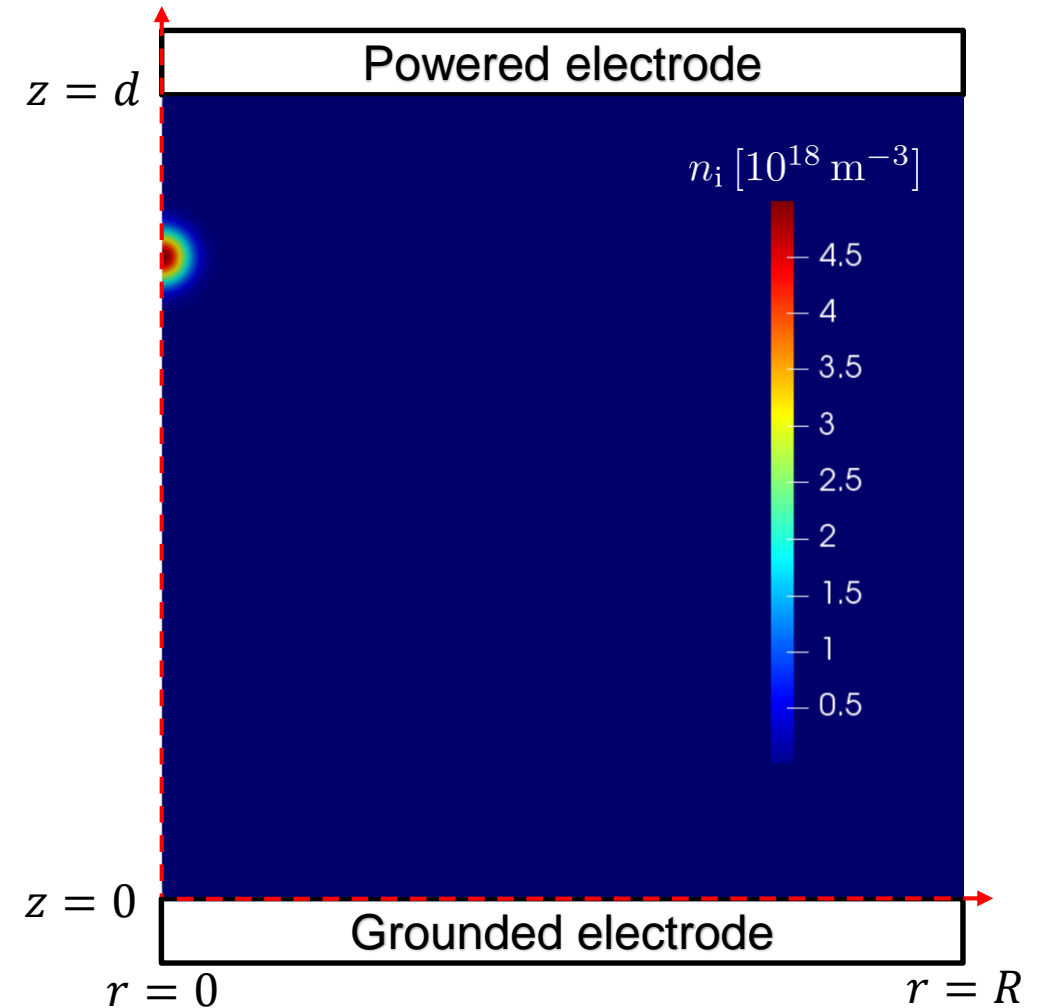
## Code verification by benchmarking

- Axisymmetric positive streamer in air at atmospheric pressure and 300 K is modelled using 2D FEDM code.
- Square domain has radius and gap distance of 1.25 cm.
- Background electric field is 15 kV/cm.
- Gaussian seed near the powered electrode is introduced to locally enhance the field and initiate the streamer.
- Mesh is refined towards the axis and streamer region (approx. 500000 elements).
- Linear Lagrange elements are used for all the equations.
- Time-step size is constant:  $\Delta t = 5$  ps.
- Temporal evolution is followed up to 12 ns (2400 time steps).



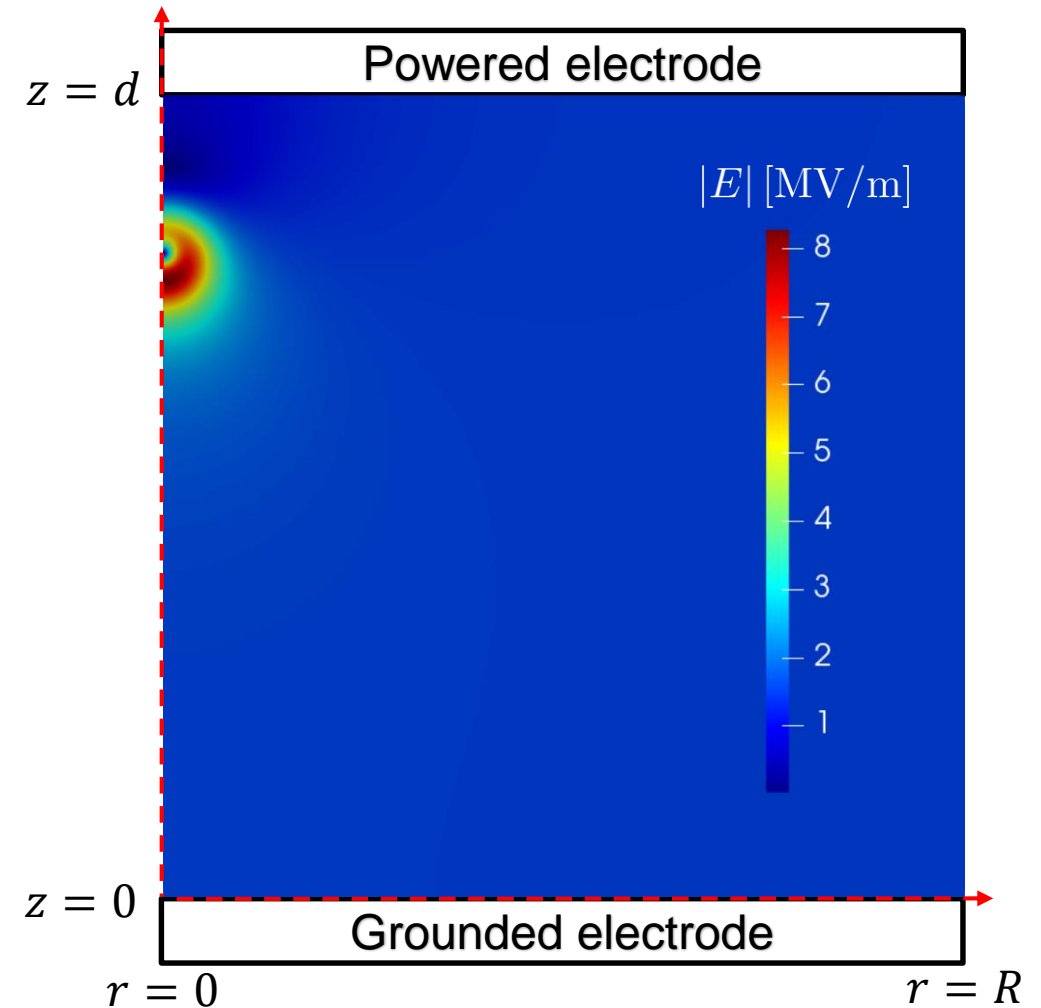
## Code verification by benchmarking

- Axisymmetric positive streamer in air at atmospheric pressure and 300 K is modelled using 2D FEDM code.
- Square domain has radius and gap distance of 1.25 cm.
- Background electric field is 15 kV/cm.
- Gaussian seed near the powered electrode is introduced to locally enhance the field and initiate the streamer.
- Mesh is refined towards the axis and streamer region (approx. 500000 elements).
- Linear Lagrange elements are used for all the equations.
- Time-step size is constant:  $\Delta t = 5$  ps.
- Temporal evolution is followed up to 12 ns (2400 time steps).



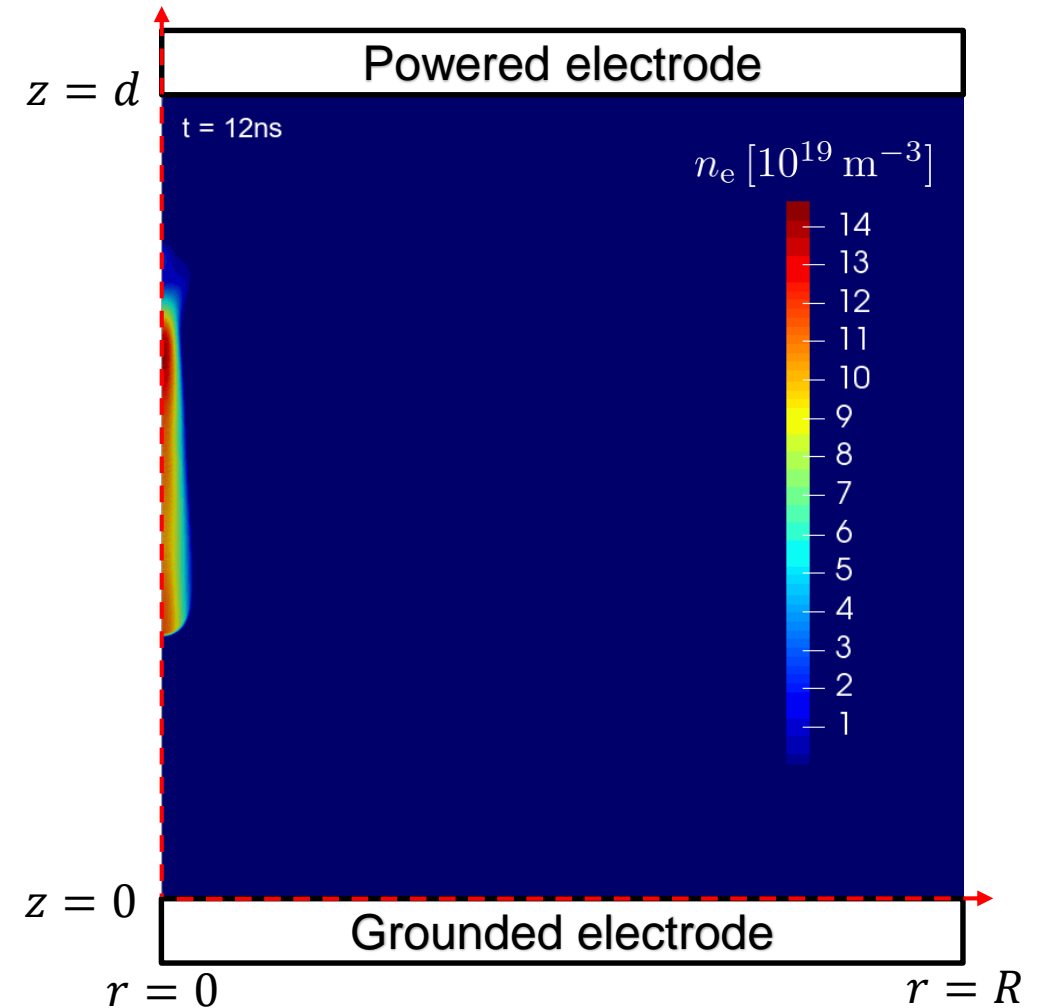
## Code verification by benchmarking

- Axisymmetric positive streamer in air at atmospheric pressure and 300 K is modelled using 2D FEDM code.
- Square domain has radius and gap distance of 1.25 cm.
- Background electric field is 15 kV/cm.
- Gaussian seed near the powered electrode is introduced to locally enhance the field and initiate the streamer.
- Mesh is refined towards the axis and streamer region (approx. 500000 elements).
- Linear Lagrange elements are used for all the equations.
- Time-step size is constant:  $\Delta t = 5$  ps.
- Temporal evolution is followed up to 12 ns (2400 time steps).



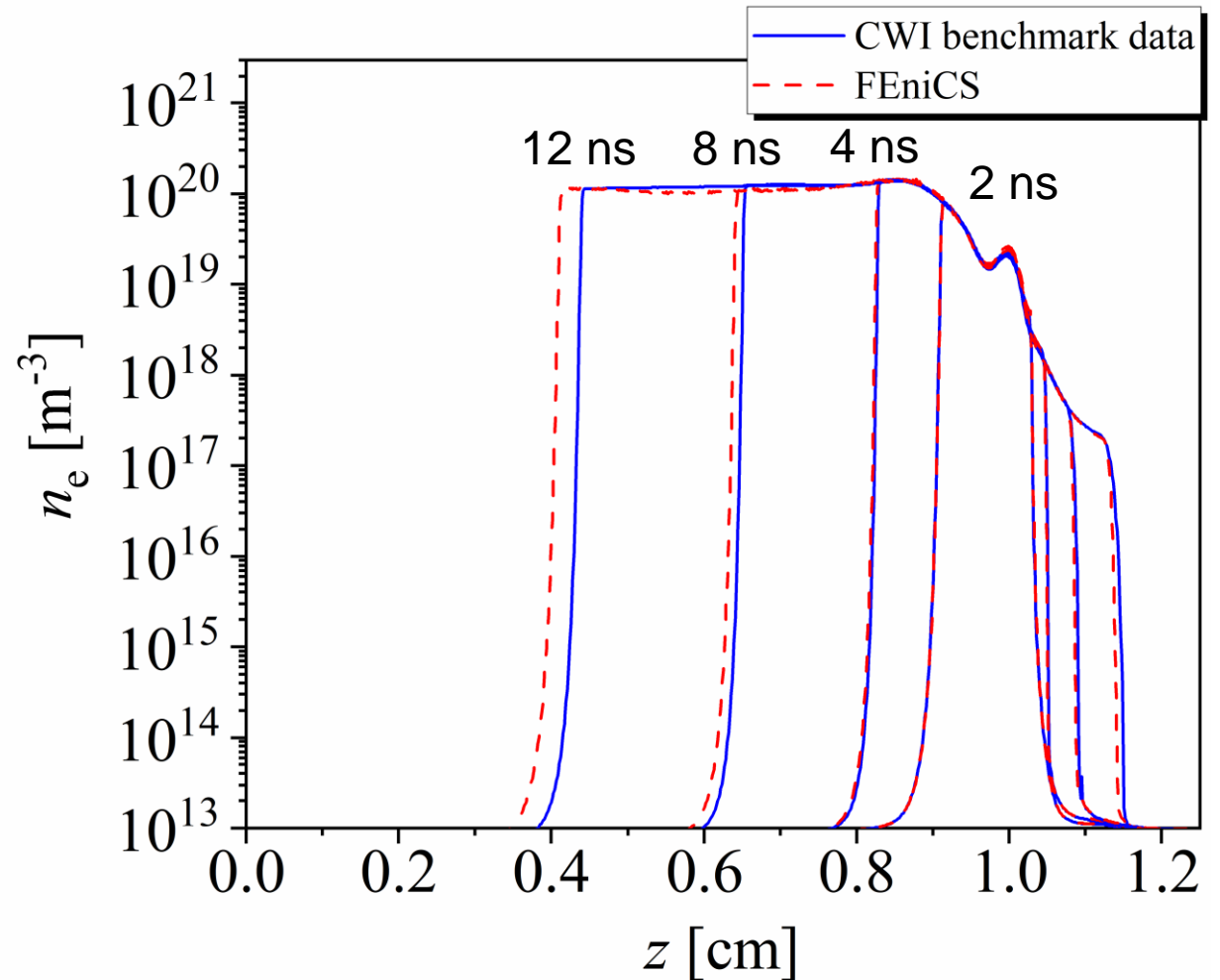
## Code verification by benchmarking

- Axisymmetric positive streamer in air at atmospheric pressure and 300 K is modelled using 2D FEDM code.
- Square domain has radius and gap distance of 1.25 cm.
- Background electric field is 15 kV/cm.
- Gaussian seed near the powered electrode is introduced to locally enhance the field and initiate the streamer.
- Mesh is refined towards the axis and streamer region (approx. 500000 elements).
- Linear Lagrange elements are used for all the equations.
- Time-step size is constant:  $\Delta t = 5$  ps.
- Temporal evolution is followed up to 12 ns (2400 time steps).



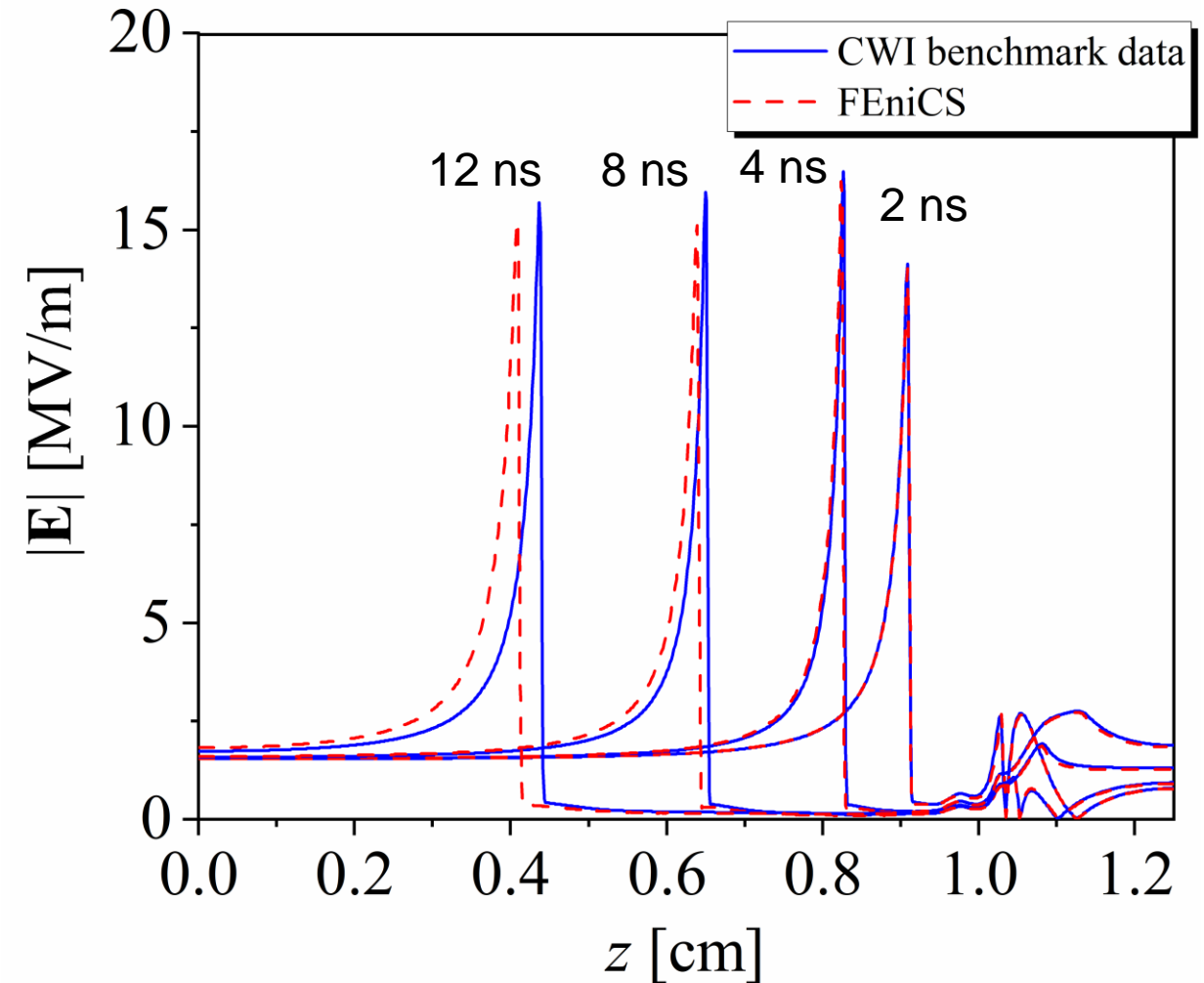
## Code verification by benchmarking

- Axisymmetric positive streamer in air at atmospheric pressure and 300 K is modelled using 2D FEDM code.
- Square domain has radius and gap distance of 1.25 cm.
- Background electric field is 15 kV/cm.
- Gaussian seed near the powered electrode is introduced to locally enhance the field and initiate the streamer.
- Mesh is refined towards the axis and streamer region (approx. 500000 elements).
- Linear Lagrange elements are used for all the equations.
- Time-step size is constant:  $\Delta t = 5$  ps.
- Temporal evolution is followed up to 12 ns (2400 time steps).



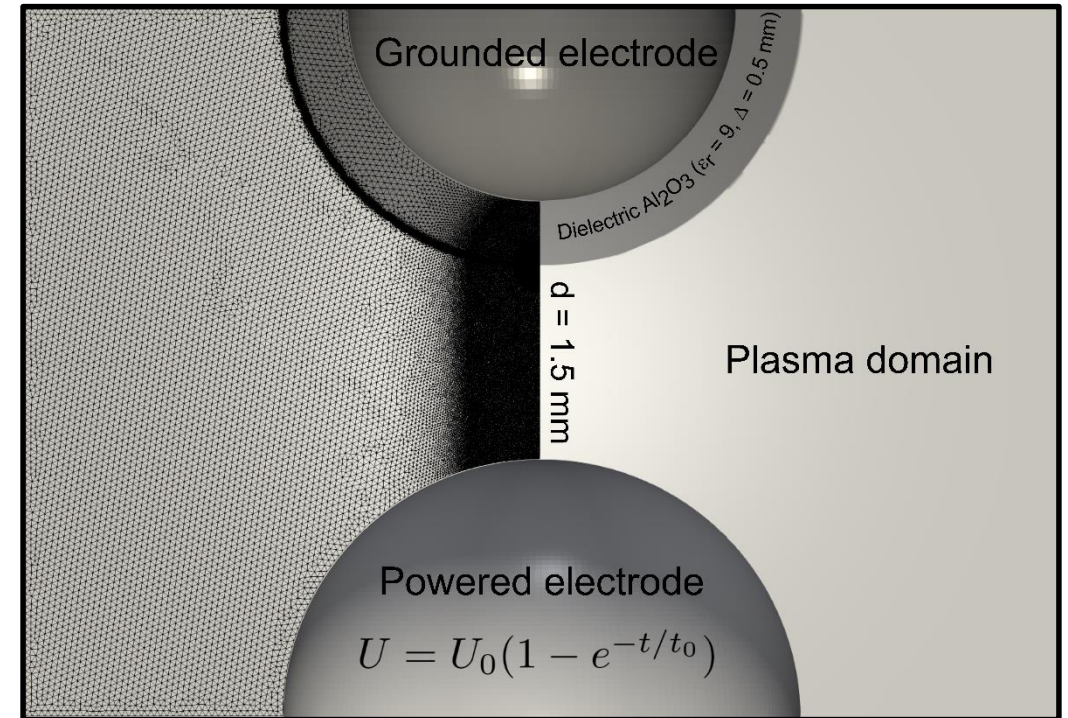
## Code verification by benchmarking

- Axisymmetric positive streamer in air at atmospheric pressure and 300 K is modelled using 2D FEDM code.
- Square domain has radius and gap distance of 1.25 cm.
- Background electric field is 15 kV/cm.
- Gaussian seed near the powered electrode is introduced to locally enhance the field and initiate the streamer.
- Mesh is refined towards the axis and streamer region (approx. 500000 elements).
- Linear Lagrange elements are used for all the equations.
- Time-step size is constant:  $\Delta t = 5$  ps.
- Temporal evolution is followed up to 12 ns (2400 time steps).



## Dielectric barrier discharge (DBD) modelling

- Atmospheric-pressure DBD in argon in asymmetric configuration is modelled using 2D FEDM code.
- Electrodes of radius 2 mm are set 1.5 mm apart.
- Grounded electrode (top) is covered by 0.5 mm thick dielectric.
- Pulsed voltage is applied to powered electrode (bottom).
- Gaussian seed near the powered electrode is introduced to locally enhance the field and initiate the streamer.
- Mesh is refined near the streamer region and along the dielectric (approx. 350000 elements).
- Linear Lagrange elements are used for all the equations.
- Adaptive time stepping is used ( $1 \text{ ps} < \Delta t < 100 \text{ ps}$ ).
- Temporal evolution is followed up to about 43 ns.



# Dielectric barrier discharge (DBD) modelling

- Atmospheric-pressure DBD in argon in asymmetric configuration is modelled using 2D FEDM code.
- Electrodes of radius 2 mm are set 1.5 mm apart.
- Grounded electrode (top) is covered by 0.5 mm thick dielectric.
- Pulsed voltage is applied to powered electrode (bottom).
- Gaussian seed near the powered electrode is introduced to locally enhance the field and initiate the streamer.
- Mesh is refined near the streamer region and along the dielectric (approx. 350000 elements).
- Linear Lagrange elements are used for all the equations.
- Adaptive time stepping is used ( $1 \text{ ps} < \Delta t < 100 \text{ ps}$ ).
- Temporal evolution is followed up to about 43 ns.

$$-\varepsilon_0 \varepsilon_r \nabla^2 \phi = \sum_p q_p n_p$$

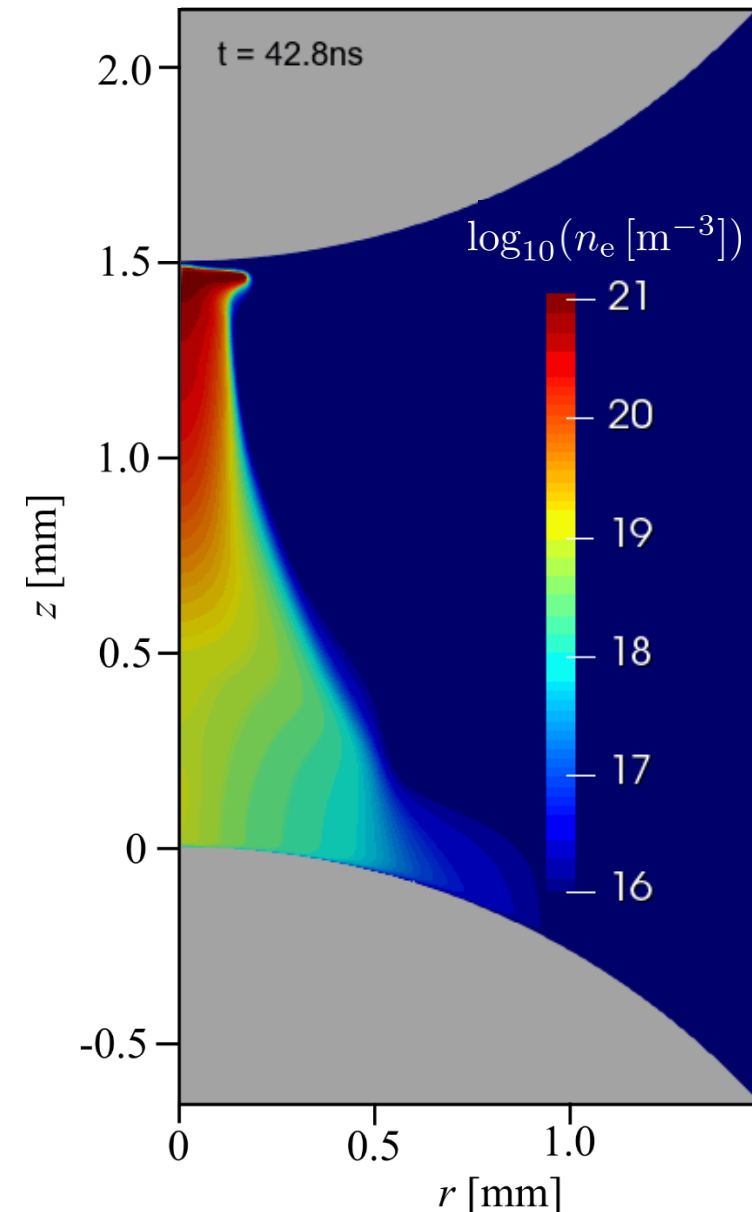
$$\frac{\partial n_p}{\partial t} + \nabla \cdot \mathbf{\Gamma}_p = S_p$$

$$\frac{\partial w_e}{\partial t} + \nabla \cdot \mathbf{Q}_e = -e_0 \mathbf{E} \cdot \mathbf{\Gamma}_e + \tilde{S}_e$$

$$\frac{\partial \sigma}{\partial t} = \sum_p q_p \mathbf{\Gamma}_p \cdot \boldsymbol{\nu}$$

## Dielectric barrier discharge (DBD) modelling

- Atmospheric-pressure DBD in argon in asymmetric configuration is modelled using 2D FEDM code.
- Electrodes of radius 2 mm are set 1.5 mm apart.
- Grounded electrode (top) is covered by 0.5 mm thick dielectric.
- Pulsed voltage is applied to powered electrode (bottom).
- Gaussian seed near the powered electrode is introduced to locally enhance the field and initiate the streamer.
- Mesh is refined near the streamer region and along the dielectric (approx. 350000 elements).
- Linear Lagrange elements are used for all the equations.
- Adaptive time stepping is used ( $1 \text{ ps} < \Delta t < 100 \text{ ps}$ ).
- Temporal evolution is followed up to about 43 ns.



## Conclusion and outlook

---

- FEDM code for automated set-up of the equations is developed.
- The code is verified using benchmarking.
- The challenges in cases where the problem is defined on several subdomains, such as DBDs, could possibly be resolved using mixed-dimensional formulation.
- Handling of electron-energy-dependent and electric-field-dependent coefficients should be further addressed because they can lead to small time-step sizes.

## Contact



Leibniz Institute for Plasma Science and Technology

Address: Felix-Hausdorff-Str. 2, 17489 Greifswald

Phone: +49 - 3834 - 554 3911, Fax: +49 - 3834 - 554 301

E-mail: [aleksandar.jovanovic@inp-greifswald.de](mailto:aleksandar.jovanovic@inp-greifswald.de), Web: [www.leibniz-inp.de](http://www.leibniz-inp.de)